Chin. Geogra. Sci. 2015 Vol. 25 No. 5 pp. 591–601
doi: 10.1007/s11769-015-0779-5

Springer Science Press
www.springerlink.com/content/1002-0063

Quantitative Analysis of Relationships Between Crack Characteristics and Properties of Soda-saline Soils in Songnen Plain, China

REN Jianhua[1, 2], LI Xiaojie[1, 3], ZHAO Kai[1, 3]

(1. *Northeast Institute of Geography and Agroecology*, *Chinese Academy of Sciences*, *Changchun* 130102, *China*; 2. *University of Chinese Academy of Sciences*, *Beijing* 100049, *China*; 3. *Changchun Jingyuetan Remote Sensing Experiment Station*, *Chinese Academy of Sciences*, *Changchun* 130102, *China*)

Abstract: The Songnen Plain has a typical soda-saline soil, which often shrinks and cracks under natural conditions during water evaporation. This study aims to analyze the relationships between the crack characteristics and the soil properties of soda-saline soils quantitatively, and attempts to establish prediction models for the main soil properties of soda-saline soils based on the results. In order to achieve these objectives, a desiccation cracking test was conducted using 17 soil specimens with different salinity levels under controlled laboratory conditions. Correlation analysis was then performed between the crack characteristics and the soil properties. The results indicate that the crack characteristics can well represent the surface appearances of cracked soils, they also can well distinguish the salinity levels of soda-saline soils while the clay contents and mineralogical compositions of soils are stable. Among the crack characteristics, crack length has the best relationships with the salinity levels of soda-saline soils. Specifically, the crack length has high correlation ($R^2 > 0.87$) with the electrical conductivity (EC), Na^+, CO_3^{2-} and the salinity, it also has reasonable relationship ($R^2 > 0.68$) with HCO_3^-, this indicates crack length can be well used for the prediction of these properties of soda-saline soils.

Keywords: soil salinization; soda-saline soil; desiccation cracking; salinity; texture features

Citation: Ren Jianhua, Li Xiaojie , Zhao Kai, 2015. Quantitative analysis of relationships between crack characteristics and properties of soda-saline soils in Songnen Plain, China. *Chinese Geographical Science*, 25(5): 591–601. doi: 10.1007/s11769-015-0779-5

1 Introduction

Soil salinization is a very severe land degradation process in arid and semi-arid regions, which strongly damages soil conditions and reduces agricultural productivity (Yang *et al*., 2010) and also poses serious economical risks. It has been reported that soil salinization has already affected approximately 7% of the earth′s surface area (Ghassemi *et al*., 1995), in addition, the affected area keeps increasing with the impacts of human activities (Lian *et al*., 2010). Therefore, it is very important and urgent to identify the salt-affected areas and determine the salinity of these soils. Most of the conventional measurement methods for the salinity of saline soils involve sampling in the field and analyzing the samples in the laboratory (Vukadinovic and Rengel, 2007; Mavi *et al*., 2012). However, conventional methods are disadvantageous due to their long measurement cycles, tedious testing processes and high labor intensity. The EM-38 has been extensively used in studies on the salt contents and distributions of soils since it can quickly reflect the salinity of soils through measuring the electrical conductivity (EC) of soils without contact. However, the EM-38 is easily affected by the physical properties of soils, such as the soil moisture content, the soil texture and the soil temperature; besides, the EM-38 is also affected by the external measurement environment during the measurement process (Zhu *et al*., 2010; Padhi

Received date: 2014-09-17; accepted date: 2015-01-14
Foundation item: Under the auspices of National Natural Science Foundation of China (No. 41201335)
Corresponding author: LI Xiaojie. E-mail: lixiaojie@iga.ac.cn

et al., 2011). With the rapid development of sensor technology, an increasing number of studies have been focusing on using the remote sensing approach to estimate the distributions and the salinity of the saline soils (Urquhart *et al*., 2012; Allbed *et al*., 2014). However, many factors can affect the electromagnetic transmission process, which is often further complicated by mixed pixel problems; in addition, most of the remote-sensing data sources have relatively large bandwidths, and thus, these data can not accurately reflect the spectral characteristics of the salt contents of soils in a specific spectral band (Metternicht and Zinck, 2003).

Under natural conditions, desiccation cracking of swelling soils is a very common phenomenon during water evaporation, which can significantly affect the soil performance in geotechnical, agricultural and environmental applications. Specifically, the cracks decrease the strength and the stability of soils, which can cause many serious damages in engineering such as slopes, road embankments, landfills and other infrastructures (Dyer *et al*., 2009; Lees *et al*., 2013; Utili, 2013). Moreover, the geometric structure of cracks changes the migration process of soil moisture, nutrients, and microbes (Romkens and Prasad, 2006). To date, studies about cracks mainly focused on the measurements of parameters of crack patterns, the influencing factors of desiccation cracking behavior and the mechanism of crack propagation process. For measurements of crack patterns, most studies focused on field measurement of cracks over the past decades (Ringrose-Voase and Sanidad, 1996; Novak, 1999). With the development of computers, more studies have focused on image processing techniques since its rapid, accurate and non-destructive advantages. Yan *et al*. (2002) extracted fractal dimension of the surface of slurry-infiltrated reinforced concrete (SIFCON), the results are shown a very positive correlation with the fiber volume content of SIFCON; Vogel *et al*. (2005) measured the angle distribution of a soil network to identify the aggregates segmented by the crack, the research suggests that the frequency distribution of angles within the crack pattern was found to be invariant which is supposed to reflect the common physical processes of crack formation; Liu *et al.* (2013) developed special software CIAS to extract the geometric characteristics of crack patterns automatically, the software shown a great potential to study the generation and development of soil crack patterns and rock fractures. In terms of understanding the influencing factors, many studies have focused on the effects of testing conditions, environmental conditions and special specimen preparations. Tang *et al*. (2008; 2011a; 2011b) conducted laboratory tests to investigate the effects of wetting-drying cycles, temperature, evaporation rate, thickness of soil layer and soil types on the initiation and evolution of cracks in clay layer. Nahlawi and Kodikara (2006) carried out five desiccation cracking tests for saturated slurries using shrinkage moulds in a humidity chamber, the results shown that the desiccation rate decreased as the layer thickness increased under similar environmental conditions. However, the study did not consider the effects of directionality on the cracking process since the lengths of the moulds were larger than their widths. Lakshmikantha *et al*. (2012) also studied the thickness factor and shown another experimental evidence of specimen size effect in soil cracking. DeCarlo and Shokri (2014) performed fractal and density correlation function analysis to study the effects of substrate particle size on the desiccation cracking process, crack length and the crack width shown the opposite tendency. Moreover, many researchers have paid attention to the modeling and simulation of the desiccation cracking process (Peron *et al*., 2009; Li and Zhang, 2011).

As is known to us, soda-saline soil is a typical type of salinized soil. Soda-saline soils have relatively high soil clay contents and strong shrinkage properties. Therefore, desiccation cracking is very common in the soda-saline areas during water evaporation. As the main chemical characteristic of salinized soils, the salt contents (especially the exchangeable cations in the soil solution) affect and reflect, to a large extent, the soil cracking process. However, there have been very few studies of the relationships between soil properties especially those related to salt contents and the characteristics of soil cracks. In the present study, the effects of different soil properties (especially those related to salinity) on the soil desiccation cracking process were investigated, the relationship between soil properties and the characteristics of soil cracks were also quantitatively analyzed. To achieve these aims, a desiccation cracking test was conducted under controlled laboratory conditions; the characteristics of crack patterns including three geometric parameters of and four gray level co-occurrence matrix (GLCM) textural features were then extracted for each specimen based on techniques of

digital image processing. Following this, correlation analysis were performed and discussed between the crack characteristics and the soil properties. Finally, prediction models were then developed for six main soil properties of soda-saline soils based on the results.

2 Materials and Methods

2.1 Study area

The Songnen Plain is located in the central region of Northeast China. Because of the inadequate drainage, high groundwater level and high mineralization, soil salinization is very severe in the Songnen Plain. The Songnen Plain is one of the major soil salinization areas in China as well as one of the three major accumulation areas of soda-saline soil in the world. The soda-saline soil of the Songnen Plain is primarily composed of $NaHCO_3$, Na_2CO_3 and NaCl with the main clay mineralogical compositions of montmorillonite, illite and kaolinite (Yan, 1988), this kind of soda saline soil largely prevents salt moving downwards due to its bad infiltration capacity, which indicates the properties of soil from the top 20 cm soil layer are very stable (Li *et al*., 2007).

2.2 Soil samples and preparation

Consideration of the effects of soil heterogeneity, 17 soil samples with various salinity levels were collected from the top 20 cm soil layer in Da′an City, which is located in the western region of Jilin Province, China. All the soil samples were obtained within a quite small region (45°29′30″–45°36′26″N, 123°47′35″–123°59′55″E).

All the soil samples were air-dried, ground and passed through a 2-mm sieve mesh. Afterward, the treated soil samples were divided into two parts. One part was used to determine the soil properties and the other part was used for the desiccation cracking experiment.

2.3 Methods

2.3.1 Soil property measurement

In the present study, the properties of the soil measured in the laboratory refer to the contents of eight main ions (Na^+, K^+, Ca^{2+}, Mg^{2+}, SO_4^{2-}, HCO_3^-, CO_3^{2-} and Cl^-), pH and EC (Bao, 2000). It is worth noting that the soda-saline soil of the Songnen Plain basically has no SO_4^{2-} content, therefore, it was neglected in this study. Soil extracts with a water/soil mass ratio of 1∶5 were used to determine the ion contents of the soil samples. In detail, the Na^+ and K^+ contents were measured using a flare photometer; the Ca^{2+} and Mg^{2+} contents were measured using the complexometric ethylene diaminete traacetic acid (EDTA) titration method; the Cl^- content was measured using the $AgNO_3$ solution titration method; the CO_3^{2-} and HCO_3^- contents were measured using the double indicator neutralization method. The pH and EC of the soil sample solutions were measured using the potentiometric method and the conductometric method, respectively (soil suspension solutions with a water/soil ratio of 1∶5 were used for the measurements). Moreover, the particle size distributions of soil samples were also measured in this study using an Mllvern MS-200 laser particle size analyzer (Eshel *et al*., 2004).

2.3.2 Desiccation cracking test

In order to produce crack patterns under controlled laboratory conditions, saturated slurry samples were prepared with mass water content of 80% using the soil samples treated previously. The obtained slurry samples were well hand-mixed and poured individually into wooden sample boxes, each with a size of 50 cm × 50 cm × 3 cm. After that, the surfaces of the slurries were flattened over the top with a spatula as the specimens, and the specimens were air-dried in the laboratory conditions until masses of all the samples no longer decreased, at which time the drying process of the soil samples was considered completed (Fig. 1).

To obtain the morphologies of the cracks of the dried soil specimens, a digital camera was then installed on a fixed experimental platform. The lens of the digital camera faced vertically downward and was 1 m above the floor; a 50 cm × 50 cm square area was determined with the projection of the camera lens on the floor as the center, which was used to ensure that the geometric distortion effect was the same for all the samples during the photographing process. Each cracked soil specimen was placed in the determined square area to be photographed. To reduce the effects of the photography environment on the photography quality, a standard colorimetric plate was used to calibrate the white balance of the camera; in addition, camera parameters such as the light sensitivity, the aperture size and the shutter speed were configured based on the light sensitivity measured by a digital photometer; before photographing, each specimen was covered with a 50 cm × 50 cm black and white mesh calibration plate and photographed, which

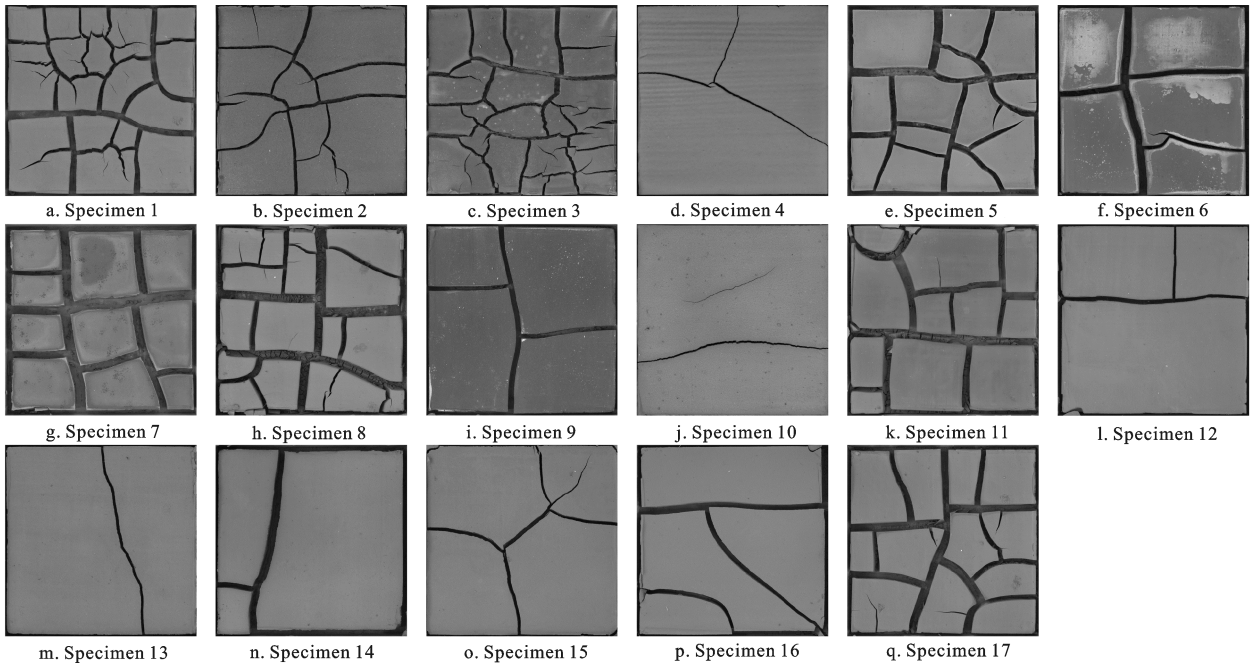

Fig. 1 Cracked soil specimens after drying process

was used for a geometric distortion correction of the crack images.

2.3.3 Crack characteristic extraction

In order to extract the geometric characteristics of crack patterns, digital image processing techniques were used in this investigation (Fig. 2). Firstly, the color photo of each specimen was geometry corrected using polynomial methods and then cropped (Fig. 2a); secondly, the color image of each cracked specimen was transformed to a grayscale image (Fig. 2b); thirdly, the grayscale image was binarizated using a gray threshold (Fig. 2c) and then inversed (Fig. 2d), indicating that the crack pattern of each specimen was segmented into aggregates (black areas) and crack areas (white areas); fourthly, the traditional open operation was performed with a given threshold of 50 pixels in order to reduce the small white spots over the aggregates, these spots were considered as the noises in the binary image (Fig. 2e); fifthly, a crack fusing method is then proposed to repair the cracks by using a given threshold of 20 pixels, to be specific, a dilation operation was applied to the binary image to eliminate the narrow space with the distance smaller than 20 pixels between the cracks (Fig. 2f); afterward, a skeletonization algorithm was operated by removing pixels from boundaries of the cracks repeatedly until one-pixel-wide skeletons of the cracks were obtained (Fig. 2g); finally, another threshold of 30 pixels was selected to clip the spurs with length smaller than 30 pixels (Fig. 2h), which were considered as noises generated during the skeletonization. Following these processes, the crack length (CL) was determined by counting pixels based on the binary skeleton of crack patterns; the crack area (CA) was extracted by computing the number of pixels representing the crack areas; the crack width (CW, defined as the radio of the crack area and the crack length) was also computed to determine the degree of soil shrinkage. It should be noted that in the present study, we selected thresholds for various soil specimens during different image processes in order to improve the accuracy. On the other hand, the crack characteristics can also be extracted using bunch mode with the same thresholds for all the soil specimens during the image processes, however, the extracted results of the crack characteristics may be less accurate.

The GLCM is a typical method for analyzing the texture features (Haralick *et al*., 1973) statistically to reflect the hue information, the local characteristics and the overall arrangement pattern of the image. The GLCM expresses the texture features of an image by calculating the second-order conditional probability densities of the gray levels of two pixels which are in a certain positional relationship in the image, $p(i, j|d, \theta)$ is used to reflect the second-order conditional probability density of gray-level pixels (i, j) in the given spatial interval d

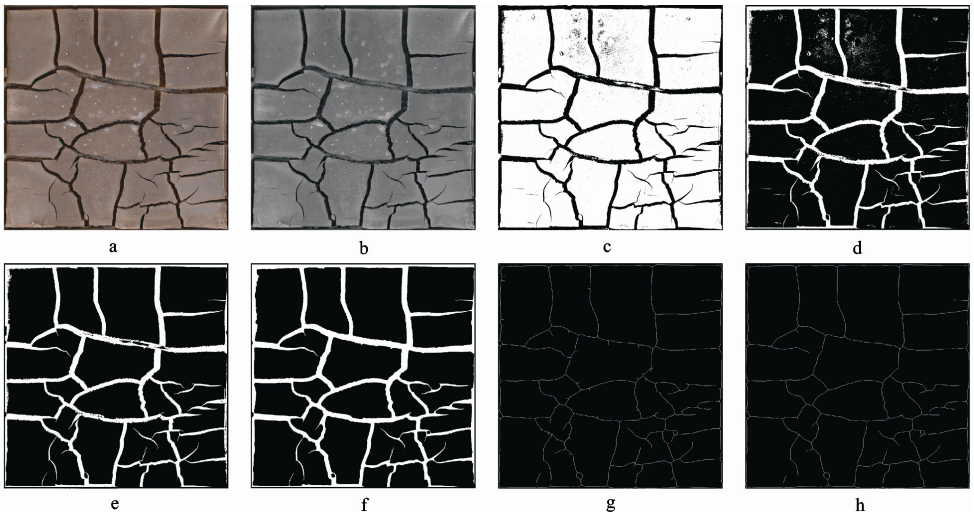

Fig. 2 Digital image processing results of crack pattern

and the direction θ. For a known gray image $f(x, y)$, the second-order conditional probability densities can be calculated using the following equation:

$$p(i,j) = g\{(x_1,y_1),(x_2,y_2) \in m \times n \mid f(x_1,y_1) = i, f(x_2,y_2) = j\} \tag{1}$$

where i, j represent the gray levels of the image $f(x, y)$ at coordinate positions (x_1, y_1) and (x_2, y_2), respectively.

In order to extract the textural features accurately, gray level of 128 and offset of one pixel were selected for computing GLCM at directions of 0°, 45°, 90° and 135°. Afterward, the GLCMs were normalized and four common used textural features (the contrast, CON; the entropy, ENT; the energy, ENE; the homogeneity, HOM) were then derived from the normalized GLCMs (Berberoglu *et al*., 2007; Ou *et al*., 2014). The CON expresses the clarity of the each image; the ENT reflects the randomness of pixel value distributions (PVD); the ENE shows the texture size and the uniformity of PVD and the HOM stands for the stability of PVD. Note that for each texture feature, characteristic values at four directions were averaged as the final texture feature to avoid the effect of directions. The detailed equations for the textural features are as the follows.

$$CON = \sum_{n}^{N_g - 1} n^2 \left\{ \sum_{i=1}^{N_g} \sum_{j=1}^{N_g} p(i,j) \right\}, |i-j| = n \tag{2}$$

$$ENT = -\sum_{i=1}^{N_g} \sum_{j=1}^{N_g} p(i,j) \log(p(i,j)) \tag{3}$$

$$ENE = -\sum_{i=1}^{N_g} \sum_{j=1}^{N_g} \{p(i,j)\}^2 \tag{4}$$

$$HOM = \sum_{i=1}^{N_g} \sum_{j=1}^{N_g} \frac{p(i,j)}{1+(i-j)^2} \tag{5}$$

where $p(i, j)$ is the value of the normalized GLCM of the image; N_g represents the gray level for the normalized GLCM.

3 Results and Analyses

3.1 Soil properties

Table 1 lists the statistical characteristics of the soil properties of soil samples. Note that the salinity represents the sum of all the ion contents in the soil solutions. From Table 1, it can be seen that all the soil samples are significant alkaline with pH ranging from 8.76 to 10.60 and the EC various from 0.09 ds/m to 3.00 ds/m. The statistical characteristics of the soil properties, such as the standard deviation (SD) and the coefficient of variation (CV), show that there are relatively large differences in the ion contents especially for the Na^+ content, HCO_3^- content, Cl^- content and CO_3^{2-} content, indicating that the selection of sample sites reflects the distribution range of soil properties very well. Table 1 also shows that the differences of clay contents between soil samples are very small (CV = 3.75%, SD = 1.05 mg/g).

3.2 Cracking characteristics

Table 2 shows the statistical characteristics of extracted

Table 1 Statistical characteristics of soil properties (n = 17)

	Min.	Max.	Mean	SD	CV (%)	Kurtosis	Skewness
pH	8.76	10.60	9.97	0.61	6.08	1.50	–1.38
EC (ds/m)	0.09	3.00	1.10	1.00	91.24	4.99	2.23
Na^+ (mg/g)	0.12	8.03	3.18	2.89	91.05	4.89	2.21
K^+ (mg/g)	0.01	0.04	0.01	0.01	56.33	5.00	2.24
Ca^{2+} & Mg^{2+} (mg/g)	0.32	1.28	0.73	0.27	37.46	4.99	2.23
HCO_3^- (mg/g)	0.61	6.34	2.24	1.47	65.50	4.88	2.20
CO_3^{2-} (mg/g)	0.00	4.62	0.69	1.15	166.42	4.99	2.23
Cl^- (mg/g)	0.08	4.10	0.87	1.17	134.46	4.99	2.23
Salinity (mg/g)	1.59	20.71	7.73	5.93	76.72	3.92	1.96
Clay (%)	26.56	29.76	27.91	1.05	3.75	–0.95	0.58
Silt (%)	30.28	40.23	35.21	3.00	8.53	–0.97	0.04
Sand (%)	31.83	42.70	37.12	3.76	10.14	–1.53	–0.02

Note: SD is standard deviation; CV is coefficient of variation

Table 2 Statistical characteristics of crack characteristics of soil specimens

	CL (cm)	CA (cm)	CW (cm)	CON	ENT	ENE	HOM
Min.	67.51	23.95	0.25	1.46	5.13	0.01	0.45
Max.	485.42	428.55	1.13	11.26	8.21	0.06	0.73
Mean	205.91	207.44	0.74	4.99	6.75	0.03	0.61
SD	118.66	140.06	0.27	3.15	0.96	0.01	0.08
CV	57.63	67.52	36.30	63.17	14.19	56.42	13.49

Note: CL, crack length; CA, crack area; CW, crack width; CON, contrast; ENT, entropy; ENE, energy; HOM, homogeneity

geometric crack characteristics from the crack patterns of the specimens. Note that CL ranges from 67.51 cm to 485.42 cm, CA ranges from 23.95 cm^2 to 428.55 cm^2, CW varies between 0.25 cm and 1.13 cm, in addition, all kinds of geometric crack parameters correspond with each other and the tendencies of all the geometric crack parameters are quite similar. Moreover, Table 2 also shows the textural characteristics extracted from the crack patterns of all the specimens. Specially, CON ranges from 1.46 to 11.26, ENT covers from 5.13 to 8.21, ENE ranges from 0.01 to 0.06 and HOM contains a range from 0.45 to 0.73, respectively. Moreover, the SD and the CV show that there are relatively large differences in the crack characteristics, indicating that the crack characteristics can distinguish the cracking degree of specimens very well.

3.3 Correlation analyses

Table 3 shows the correlation analysis results between crack characteristics and soil properties of all the specimens. It can be seen that the geometric characteristics of crack patterns have positive relationships with the soil properties. Among the geometric characteristics, the CL has overall highest correlation coefficients (R-values) with soil properties, for example, the CL is highly correlated with EC, Na^+, HCO_3^-, CO_3^{2-} and salinity (R > 0.82). For the textural characteristics, CON and ENT have positive relationships with all the soil properties; on the other hand, the relationships between soil properties and ENE, HOM show the opposite tendency. It is worth noting that compared with other textural characteristics, ENT has the strongest relationships with the soil properties especially for EC, Na^+ and salinity (R > 0.77). It can also be seen from Table 3 that although the relationships between soil properties and textural characteristics are poor compared with crack length, the textural characteristics can show an overall statistical feature of the surface of cracked soil specimens rather than the geometric characteristics and offer a new method to describe the soil cracks quantitatively.

3.4 Soil properties prediction

In order to illustrate the potential of soil property predictions of soda-saline soils, CL was selected as the optimal crack characteristic to draw scatter diagrams with the soil chemical properties of specimens (Fig. 3).

Table 3 Correlation coefficients between crack characteristics and main soil properties

	pH	EC	Na^+	K^+	Ca^{2+} & Mg^{2+}	HCO_3^-	CO_3^{2-}	Cl^-	Salinity	Clay
CL	0.73*	0.96*	0.93*	0.22	0.56*	0.82*	0.86*	0.63*	0.97*	0.14
CA	0.63*	0.76*	0.74*	0.10	0.13	0.61*	0.45*	0.69*	0.73*	0.43*
CW	0.36	0.35	0.34	0.05	–0.20	0.33	0.05	0.37	0.32	0.54*
CON	0.62*	0.74*	0.74*	0.61*	0.68*	0.64*	0.69*	0.32	0.75*	0.16
ENT	0.52*	0.79*	0.77*	0.30	0.59*	0.60*	0.56*	0.56*	0.77*	0.10
ENE	–0.45*	–0.74*	–0.70*	–0.29	–0.59*	–0.52*	–0.49*	–0.55*	–0.70*	–0.07
HOM	–0.35	–0.68*	–0.69*	–0.43*	–0.77*	–0.42*	–0.59*	–0.44*	–0.68*	–0.01

Notes: *, significant at the 0.05 level. EC, electrical conductivity; CL, crack length; CA, crack area; CW, crack width; CON, contrast; ENT, entropy; ENE, energy; HOM, homogeneity

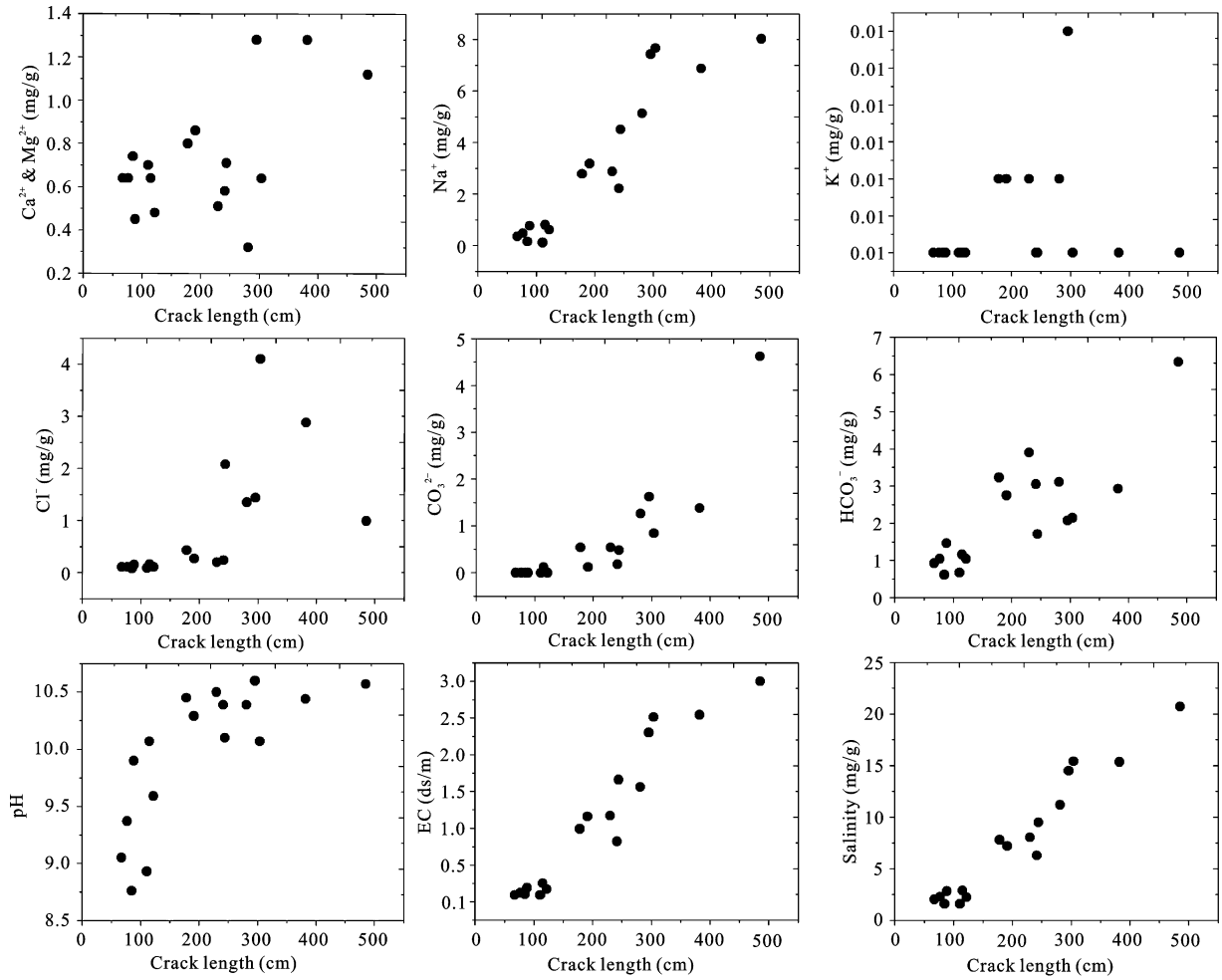

Fig. 3 Scatter diagrams between crack length and soil chemical properties

It can be seen that for Na^+, EC and salinity, the linear relationships are obvious among the data points; for HCO_3^-, the data points also show linear distribution but are quite disperse; for pH and CO_3^{2-}, the distributions of the data points conform to the trend of quadratic curves; however, for K^+, Ca^{2+} & Mg^{2+} and Cl^-, there is of no regularity for the distributions of the data points. The optimal fitting curves, therefore, were then developed between CL and six main soil properties according to the scatter analysis results (Fig. 4). For Na^+, HCO_3^-, EC and salinity, linear models are developed; for pH and CO_3^{2-}, polynomial regression models are developed.

To quantity performance of the regression models, various evaluation indexes such as coefficient of determination (R^2), root mean square error (RMSE), relative root mean square error (RMSE, %), mean absolute error (MAE), relative mean absolute error (MAE, %) and predicted ratio of deviation (PRD) were calculated (Table 4). According to the evaluation standard (Farifteh *et al*., 2007), the regression models can be considered accurate for EC, CO_3^{2-} and salinity since both R^2 is higher than 0.91 and RPD is higher than 2.5, respectively, however high relative RMSE (%) and relative MAE (%) indicate the estimated CO_3^{2-} are less stable and reliable comparatively, this is because more random errors generate during polynomial modeling rather than linear modeling; the regression model of Na^+ can be considered good since both the RPD is higher than 0.82 and the R^2 varies between 0.81 and 0.90; for the predictions of HCO_3^- and pH, the models can be considered only approximate since the R^2 lies between 0.66–0.81 and the RPD is higher than 1.5, moreover, the stability and reliability of the prediction models for pH and HO_3^- are quite poor due to the high relative root mean square errors.

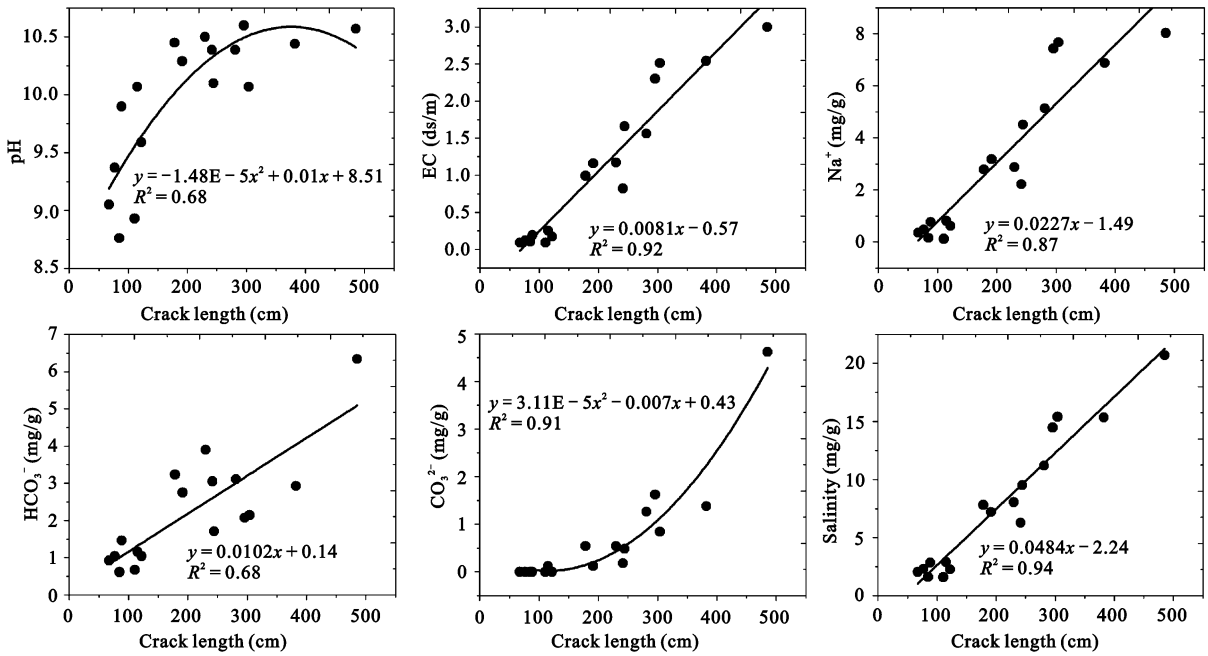

Fig. 4 Optimal fitting curves between crack length and main soil properties

Table 4 Evaluation indexes of optimal fitting results for different soil properties

	R^2	RMSE	RMSE (%)	MAE	MAE (%)	PRD
pH	0.68	3.32	36.88	0.34	3.46	24.09
EC	0.92	0.28	25.56	0.21	19.39	4.03
Na^+	0.87	1.04	32.59	0.77	24.23	2.40
HCO_3^-	0.68	0.81	36.10	0.67	30.08	2.05
CO_3^{2-}	0.91	0.31	46.35	0.22	32.48	3.94
Salinity	0.94	1.44	18.61	1.11	14.34	4.48

Note: RMSE is root mean square error; MAE is mean absolute error; PRD is predicted ratio of deviation

4 Discussion

In this study, the specific courses of desiccation cracking of slurry specimens are described as follows: firstly, the supernatant water evaporated from the surface of the initial fully saturated slurry soil specimens; secondly, capillary suction gradually developed between soil particles in the upper layer of specimens; thirdly, once the surface tensile stress induced by the increasing capillary suction exceeded the bonding tensile strength of soil particles, cracks occurred on soil surface at some random locations and developed freely, these cracks were regarded as the main cracks; after that, the main cracks began to develop branches and these derived cracks propagated perpendicular to the main cracks, the derived cracks also branched in the same way until the surface energy of the soil specimens reached stability; finally, no more cracks were generated on the soil surface while the aggregations continued shrinking until the drying process completed. Studies indicated the desiccation cracking undergoing a drying process is controlled by physical properties of soils such as soil suction, tensile stress, shear strength, tensile strength and specific surface energy, and tensile stress and tensile strength are the direct influencing factors among these properties (Amarasiri *et al*., 2011; Trabelsi *et al*., 2012). Many researches have illustrated that these physical properties above are mainly dependent on the clay content and the mineralogical compositions of the clay (Bovin *et al*., 2004; Hallett and Newson, 2005). Notably, for the desiccation cracking test of soil specimens, these listed physical properties of soils are also affected by the various environmental factors, the controlled laboratory conditions and the specimen selections. However, all the specimens in this investigation were all obtained within a quite narrow landscape and the clay content were nearly the same (Table 1) and the clay mineralogical compositions also kept the same in the study area (Li and Wang, 2006). Moreover, the effects of laboratory conditions including relative humidity, temperature and the specifications of specimens were also the same for the specimens in this study. The soil properties related to salinity, therefore, influenced the initiation and propaga-

tion and of the desiccation cracks. To be specific, this is because all the specimens were over saturated with water content of 80% at the beginning, during the desiccation cracking process, combined water films were formed generally among the soil particles under the interaction between soil colloidal particles and exchangeable cations, and the thickness of those combined water films increased with the contents of exchangeable cations of the soil specimens. The formed water films dispersed the cementation and increased the spacing of soil particles，which reduced the tensile strength and the shear strength between soil colloidal particles (Zhang *et al*., 2008). Furthermore, the lubrication of salt solution also decreased the shear strength among soil particles (Aksenov *et al*., 2003; Jeong *et al*., 2012).

Table 3 indicates Na^+ is highly correlated to the crack characteristics; this is because Na^+ is the main component of combined water films between soil particles, in addition, Na^+ has a very large hydrolytic radius and the content of Na^+ is far greater than the other cations in the soil solution. It can also be seen from Table 3 and Fig. 3 that the EC and salinity have little higher correlation coefficients with the crack characteristics compared with Na^+ since the contribution of other exchangeable cations. The relationships between Cl^-, HCO_3^-, CO_3^{2-}, pH and the crack characteristics are relatively poor, this is because Cl^-, HCO_3^- and CO_3^{2-} occupied a certain proportion in the soil solution; the pH, in addition, was determined by the content of OH^- hydrolyzed from HCO_3^- and CO_3^{2-}, however the hydrolysis of HCO_3^- and CO_3^{2-} was incomplete. The results of correlation analysis also show that the relationships between GLCM texture features and soil properties are poor compared with CL and CA. This is because salt crystals were forming at the surface of specimens randomly with water evaporation during the desiccation cracking process and the cracks on the surface of specimens also occurred randomly on the surface of soil specimens, which made GLCM texture features not stable as geometric characteristics (CL and CA). On the other hand, as a measure of soil shrinkage, CW has a positive relationship with the clay content since the clay content is related to the shrinkage capacity of soils (Bovin *et al*., 2004), however the relationship is not remarkable due to the slight difference of clay content between various soil samples.

5 Conclusions

In this study, a desiccation cracking test was conducted for the soda-saline soil samples with different salinity levels obtained from Da′an City, located in Songnen Plain, west of Jilin Province, China. The physicochemical properties of the soil samples were measured; seven crack characteristics including three geometric parameters and four GLCM statistical texture features were also extracted; a correlation analysis was then performed and discussed between these crack characteristics and the soil properties; afterward predictive models were developed between the optimal crack characteristic CL and six main soil properties (pH, EC, Na^+, HCO_3^-, CO_3^{2-}, and salinity). The main conclusions are as follows:

(1) The crack characteristics extracted by image processing techniques can well quantify the desiccation cracking process and distinguish the surface appearances of cracked soils with different soil properties. (2) The contents of exchangeable cations (reflect the salinity levels of soda-saline soils) influence the initiation and propagation of desiccation cracking process to a great degree while the clay content and the mineralogical compositions of the soda-saline soil specimens are of little difference. (3) The crack characteristics show quite great potentials and can be well used for the predictions of soil properties especially for Na^+, EC, total salinity and CO_3^{2-}. Among the crack characteristics, crack length is the optimal one for soil property predictions.

References

Aksenov V I, Kal′bergenov R G, Leonov A R, 2003. Strength characteristics of frozen saline soils. *Soil Mechanics and Foundation Engineering*, 40(2): 55–59. doi: 10.1023/A:1024436118466

Allbed A, Kumar L, Aldakheel Y Y, 2014. Assessing soil salinity using soil salinity and vegetation indices derived from IKONOS high-spatial resolution imageries: application in a date palm dominated region. *Geoderma*, 230–231: 1–8. doi: 10.1016/j.geoderma.2014.03.025

Amarasiri A L, Kodikara J K, Costa S, 2011. Numerical modeling of desiccation cracking. *International Journal for Numerical and Analytical Methods in Geomechanics*, 35(1): 82–96. doi: 10.1002/nag.894

Bao Shidan, 2000. *Agricultural Chemistry Analysis of Soils*. Beijing: Chinese Agriculture Press, 152–200. (in Chinese)

Berberoglu S, Curran P J, Lloyd C D, 2007. Texture classification of Mediterranean land cover. *International Journal of Applied*

Earth Observation and Geo-information, 9(3): 322–334. doi: 10.1016/j.jag.2006.11.004

Bovin P, Garnier P, Tessier D, 2004. Relationship between clay content, clay type and shrinkage properties of soil samples. *Soil Science Society of America Journal*, 68(4): 1145–1153. doi: 10.2136/sssaj2004.1145

DeCarlo K F, Shokri N, 2014. Effects of substrate on cracking patterns and dynamics in desiccating clay layers. *Water Resources Research*, 50(4): 3039–3051. doi: 10.1002/2013WR014466

Dyer M, Utili S, Zielinski M, 2009. Field survey of desiccation fissuring of flood embankments. *Proceedings of the ICE-Water Management*, 162(3): 221–232. doi: 10.1680/wama.2009.162.3.221

Eshel G, Levy G J, Mingelgrin U *et al*., 2004. Critical evaluation of the use of laser diffraction for particle-size distribution analysis. *Soil Science of America Journal*, 68(3): 736–743. doi: 10.2136/sssaj2004.7360

Farifteh J, Van der Meer F, Atzberger C *et al*., 2007. Quantitative analysis of salt-affected soil reflectance spectra: a comparison of two adaptive methods (PLSA and ANN). *Remote Sensing of Environment*, 110(1): 59–78. doi: 10.1016/j.rse.2007.02.005

Ghassemi F, Jakeman A J, Nix H A, 1995. *Salinisation of Land and Water Resources*: *Human Causes*, *Extent*, *Management and Case Studies*. *The Australian National University*/*CAB Internatinal*. Canberra, Australia.

Hallett P D, Newson T A, 2005. Describing soil crack formation using elastic-plastic fracture mechanics. *European Journal of Soil Science*, 56(1): 31–38. doi: 10.1111/j.1365-2389.2004.00652.x

Haralick R M, Shamugam K, Dinstein I, 1973. Texture features for image classification. *IEEE Transaction on Systems*, *Man*, *and Cybernetics*, 3(6): 610–621. doi: 10.1109/TSMC.1973.4309314

Jeong S W, Locat J, Leroueil S, 2012. The effects of salinity and shear history on the rheological characteristics of illite-rich and Na-montmorillonite-rich clays. *Clay Mineral Society*, 60(2): 108–120. doi: 10.1346/CCMN.2012.0600202

Lakshmikantha M R, Prat P C, Ledesma A, 2012. Experimental evidence of size effect in soil cracking. *Canadian Geotechnical Journal*, 49(3): 264–284. doi: 10.1139/t11-102

Lees A S, MacDonald G J, SheermanChase A *et al*., 2013. Seasonal slope movements in an old clay fill embankment dam. *Canadian Geotechnical Journal*, 50(5): 503–520. doi: 10.1139/cgj-2012-0356

Li Bin, Wang Zhichun, 2006. The alkaline characteristics and influencing factors of soda saline-alkali soils in Songnen Plain. *Journal of Arid Land Resources and Environment*, 20(6): 183–191. (in Chinese)

Li Bin, Wang Zhichun, Liang Zhengwei *et al*., 2007. Relationships between parameters of sodic saline soils in Da′an City of Jilin Province. *Chinese Journal of Soil Science*, 38(3): 443–446. (in Chinese)

Li J, Zhang L, 2011. Study of desiccation crack initiation and development at ground surface. *Engineering Geology*, 123(4): 347–358. doi: 10.1016/j.enggeo.2011.09.01

Lian Yi, Wang Jie, Tu Gang *et al*., 2010. Quantitative assessment of impacts of regional climate and human activities on saline-alkali land changes: a case study of Qian′an County, Jilin Province. *Chinese Geographical Science*, 20(1): 91–97. doi: 10.1007/s11769-010-0091-3

Liu C, Tang C, Shi B *et al*., 2013. Automatic quantification of crack patterns by image processing. *Computer & Geosciences*, 57: 77–80. doi: 10.1016/j.cageo.2013.04.008

Mavi M S, Marschner P, Chittleborough D J *et al*., 2012. Salinity and sodicity affect soil respiration and dissolved organic matter dynamics differentially in soils varying in texture. *Soil Biology & Biochemistry*, 45: 8–13. doi: 10.1016/j.soilbio.2011.10.003

Metternicht G I, Zinck J A, 2003. Remote sensing of soil salinity: potentials and constraints. *Remote Sensing of Environment*, 85(1): 1–20. doi: 10.1016/S0034-4257(02)00188-8

Nahlawi H, Kodikara J K, 2006. Laboratory experiments on desiccation cracking of thin soil layers. *Geotechnical and Geological Engineering*, 24(6): 1641–1664. doi: 10.1007/s10706-005-4894-4

Novak V, 1999. Soil-crack characteristics-estimation methods applied to heavy soil in the NOPEX area. *Agricultural and Forest Meteorology*, 98–99(31): 501–507. doi: 10.1016/S0168-1923(99)00119-7

Ou X, Pan W, Xiao P, 2014. In vivo skin capacitive imaging analysis by using grey level co-occurrence matrix (GLCM). *International Journal of Pharmaceutics*, 460(1–2): 28–32. doi: 10.1016/j.ijpharm.2013.10.024

Padhi J, Misra R K, 2011. Sensitivity of EM38 in determining soil water distribution in an irrigated wheat field. *Soil & Tillage Research*, 117: 93–102. doi: 10.1016/j.still.2011.09.003

Peron H, Laloui L, Hueckel T *et al*., 2009. Desiccation cracking of soils. *European Journal of Environmental and Civil Engineering*, 13(7–8): 869–888. doi: 10.1080/19648189.2009.9693159

Ringrose-Voase A J, Sanidad W B, 1996. A method for measuring the development of surface cracks in soils: application to crack development after lowland rice. *Geoderma*, 71(3–4): 245–261. doi: 10.1016/0016-7061(96)00008-0

Romkens M J M, Prasad S N, 2006. Rain infiltration into swelling/shrinking/cracking soils. *Agricultural Water Management*, 86(1–2): 196–205. doi: 10.1016/j.agwat.2006.07.012

Tang C, Liu C, Zhao L *et al*., 2008. Influencing factors of geometrical structure of surface shrinkage cracks in clayey soils. *Engineering Geology*, 101(3–4): 204–217. doi: 10.1016/j.enggeo.2008.05.005

Tang C, Cui Y, Shi B *et al*., 2011a. Desiccation and cracking behaviour of clay layer from slurry state under wetting-drying cycles. *Geoderma*, 166(1): 111–118. doi: 10.1016/j.geoderma.2011.07.018

Tang C, Shi B, Liu C *et al*., 2011b. Experimental characterization of shrinkage and desiccation cracking in thin clay layer. *Applied Clay Science*, 52(1–2): 69–77. doi: 10.1016/j.clay.2011.01.032

Trabelsi H, Jamei M, Zenzri H *et al*., 2012. Crack patterns in clayey soils: experiments and modeling. *International Journal for Numerical and Analytical Methods in Geomechanics*, 36(11): 1410–1433. doi: 10.1002/nag.1060

Urquhart E A, Zaitchik B F, Hoffman M J *et al*., 2012. Remote sensed estimates of surface salinity in the Chesapeake Bay: a statistical approach. *Remote Sensing of Environmet*, 123: 522–531. doi: 10.1016/j.rse.2012.04.008

Utili S, 2013. Investigation by limit analysis on the stability of slopes with cracks. *Geotechnique*, 63(2): 140–154. doi: 10.1680/geot.11.P.068

Vogel H J, Hoffmann H, Roth K, 2005. Studies of crack dynamics in clay soil: I. Experimental methods, results, and morphological quantification. *Geoderma*, 125(3–4): 203–211. doi: 10.1016/j.geoderma.2004.07.009

Vukadinovic V, Rengel Z, 2007. Dynamics of sodium in saline and sodic soils. *Communications in Soil Science and Plant Analysis*, 38(15–16): 2077–2090. doi: 10.1080/00103620701548811

Yan A, Wu K, Zhang X, 2002. A quantitative study on the surface crack pattern of concrete with high content of steel fiber. *Cement and Concrete Research*, 32(9): 1371–1375. doi: 10.1016/S0008-8846(02)00788-3

Yan Qiulan, 1988. The clay mineral compositions of reserve of momoge in Songnen Plain and its paleogeographic implications. *Scientia Geographica Sinica*, 8(3): 264–270. (in Chinese)

Yang Jiuchun, Zhang Shuwen, Li Ying *et al*., 2010. Dynamics of saline-alkali land and its ecological regionalization in western Songnen Plain, China. *Chinese Geographical Science*, 20(2): 159–166. doi: 10.1007/s11769-010-0159-0

Zhang Guohui, Li Jianpeng, Yu Qingchun *et al*., 2008. Effects of Salinity on shear strength of saline alkali soils in Songnen Plain. *The Chinese Journal of Geological Hazard and Control*, 19(1): 128–131. (in Chinese)